

Using reflection and transmission coefficients to retrieve surface parameters for an anisotropic metascreen: With a discussion on conversion between TE and TM polarizations

Cite as: J. Appl. Phys. 125, 095102 (2019); <https://doi.org/10.1063/1.5050987>

Submitted: 04 August 2018 . Accepted: 12 February 2019 . Published Online: 01 March 2019

Christopher L. Holloway , Edward F. Kuester , and Abdulaziz H. Haddab 



View Online



Export Citation



CrossMark

Ultra High Performance SDD Detectors



See all our XRF Solutions

Using reflection and transmission coefficients to retrieve surface parameters for an anisotropic metascreen: With a discussion on conversion between TE and TM polarizations

Cite as: J. Appl. Phys. **125**, 095102 (2019); doi: [10.1063/1.5050987](https://doi.org/10.1063/1.5050987)

Submitted: 4 August 2018 · Accepted: 12 February 2019 ·

Published Online: 1 March 2019



View Online



Export Citation



CrossMark

Christopher L. Holloway,^{1,a)} Edward F. Kuester,² and Abdulaziz H. Haddab²

AFFILIATIONS

¹National Institute of Standards and Technology (NIST), Boulder, Colorado 80305, USA

²Department of Electrical, Computer and Energy Engineering, University of Colorado, Boulder, Colorado 80309, USA

^{a)}christopher.holloway@nist.gov

ABSTRACT

In recent work, we derived generalized sheet transition conditions (GSTCs) for electromagnetic fields at the surface of a metascreen (a metasurface with a “fishnet” structure, i.e., a periodic array of arbitrary spaced apertures in a relatively impenetrable surface). The effective electric and magnetic surface susceptibilities and surface porosities that appear explicitly in the GSTCs are uniquely defined and as such serve as the physical quantities that most appropriately characterize the metascreen. These surface parameters are related to the geometry of the apertures that constitute the metascreen and can exhibit anisotropic properties if this geometry is sufficiently asymmetric. These anisotropic properties can result in mode conversion between transverse electric (TE) and transverse magnetic (TM) polarizations when a plane-wave is incident onto a metascreen. Here, we use these GSTCs to derive the plane-wave reflection (R) and transmission (T) coefficients of an anisotropic metascreen, in which the coupling between TE and TM polarizations is illustrated. These expressions for R and T are used to develop a retrieval approach for determining the uniquely defined effective surface susceptibilities and surface porosities that characterize the metascreen from measured or simulated data. We present an example of a metascreen whose apertures are filled with a high-contrast dielectric, which shows interesting resonances at frequencies where no resonances exist when the apertures are not filled.

<https://doi.org/10.1063/1.5050987>

I. INTRODUCTION

The simplicity and relative ease of fabrication of metasurfaces (surface or two-dimensional, versions of three-dimensional metamaterials) makes them attractive alternatives to metamaterials; in many applications, metasurfaces can be used in place of metamaterials.^{1,2} Any periodic two-dimensional structure whose thickness and periodicity are small compared to the wavelengths in the surrounding media is referred to as a metasurface. The distinction between a metasurface and a frequency-selective surface (FSS) is discussed in detail in Ref. 1. Within the general designation of metasurfaces, we can identify two important subclasses: metasurfaces that have a “cermet” topology, which refers to an array of isolated (non-touching) scatterers, are called metafilms [see Fig. 1(a)

for a metafilm composed of an array of spherical particles], a term coined in Ref. 3 for such surfaces. Metasurfaces with a “fishnet” structure are called metascreens.^{1,4} Metascreens are characterized by periodically spaced apertures in an otherwise relatively impenetrable surface [see Fig. 1(b) for a metascreen composed of an array of square apertures]. Other kinds of metasurfaces exist that lie somewhere between these two extremes. For example, a grating of parallel conducting wires (a metagrating) behaves like a metafilm to electric fields perpendicular to the wire axis and like a metascreen for electric fields parallel to the wire axis.⁵

The traditional and most convenient method by which to model metamaterials is with effective-medium theory, using the bulk electromagnetic parameters μ_{eff} and ϵ_{eff} . Attempts to use a similar bulk-parameter model for metasurfaces have been less

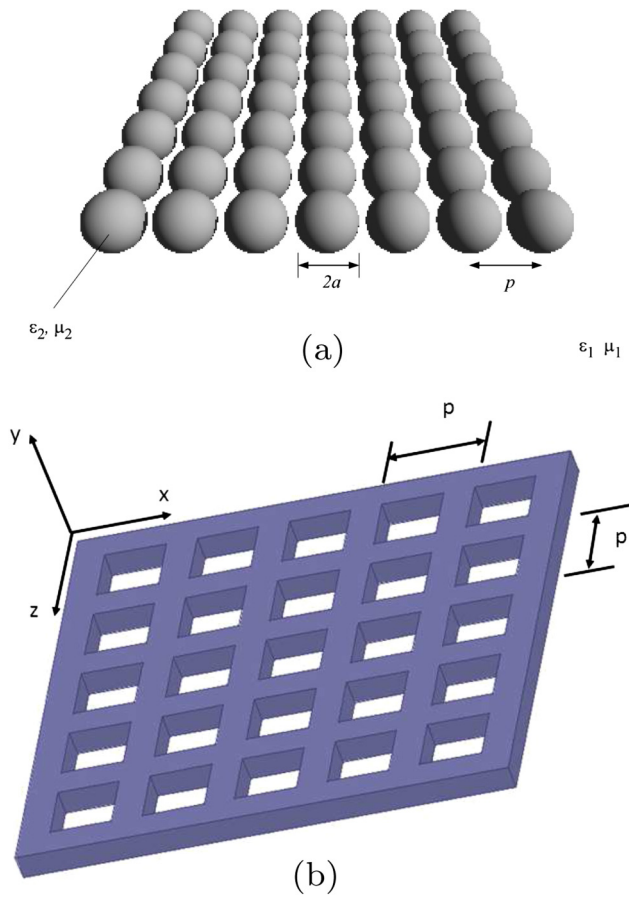


FIG. 1. Illustration of types of metasurfaces: (a) metafilm that consists of an array of spherical particles placed on the xz -plane and (b) metascreen that consists of an array of square apertures in a conducting screen located in the xz -plane.

successful. Detailed discussions of this point for metafilms have been given in Refs. 1, 6, and 7. It has been shown^{1,3,4,6-8} that the surface susceptibilities of a metafilm (or the surface porosities and susceptibilities of a metascreen) are the properties that uniquely characterize the metasurface and, as such, serve as its most appropriate descriptive parameters. As a result, scattering by a metasurface (metafilm or metascreen) is best characterized by generalized

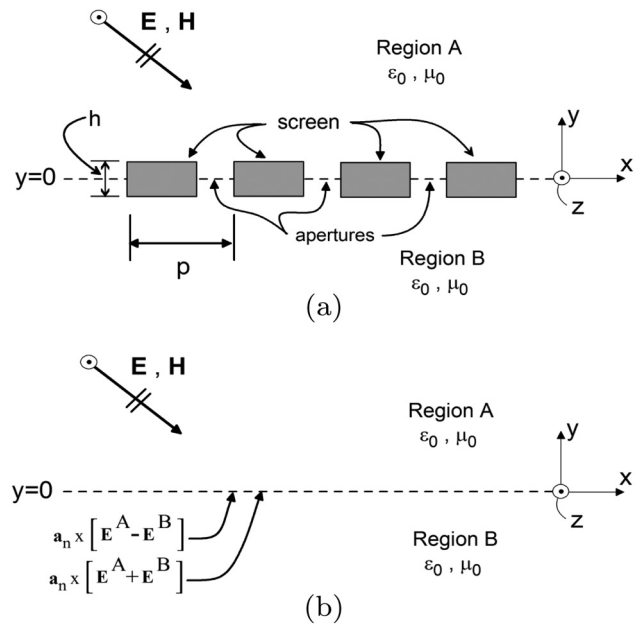


FIG. 2. (a) Metascreen (array of apertures in a conducting screen) and (b) the reference plane at which the GSTCs are applied.

sheet-transition conditions (GSTCs)^{3,4,6-8} in contrast to the effective-medium description used for a metamaterial. The coefficients appearing in the GSTCs for any given metasurface are all that are required to model its macroscopic interaction with an electromagnetic field.

While GSTCs for metafilms have been around for a few years,^{3,6-8} GSTCs for a metascreen were only recently derived.⁴ The GSTCs for a metascreen allow this surface distribution of apertures to be replaced with a boundary condition that is applied across an infinitely thin equivalent surface (hence the name metascreen), as indicated in Fig. 2. The size, shape, and spacing of the apertures are incorporated into this boundary condition through the effective surface susceptibilities and surface porosities on the interface. It was shown in Ref. 4 that the GSTCs relating the electromagnetic fields on both sides of the metascreen shown in Fig. 2 are [note that $\exp(j\omega t)$ time dependence is assumed throughout the paper]

$$\begin{aligned}
 \mathbf{a}_y \times [\mathbf{E}^A(\mathbf{r}_0) - \mathbf{E}^B(\mathbf{r}_0)] &= -\mathbf{a}_x j\omega\mu_0 \left[\chi_{MS}^{Axx} H_x^A(\mathbf{r}_0) + \chi_{MS}^{Bxx} H_x^B(\mathbf{r}_0) + \chi_{MS}^{Azz} H_z^A(\mathbf{r}_0) + \chi_{MS}^{Bzz} H_z^B(\mathbf{r}_0) \right] \\
 &\quad - \mathbf{a}_z j\omega\mu_0 \left[\chi_{MS}^{Azx} H_x^A(\mathbf{r}_0) + \chi_{MS}^{Bzx} H_x^B(\mathbf{r}_0) + \chi_{MS}^{Azz} H_z^A(\mathbf{r}_0) + \chi_{MS}^{Bzz} H_z^B(\mathbf{r}_0) \right] \\
 &\quad - \mathbf{a}_y \times \left[\chi_{ES}^{Ayy} \nabla_t E_y^A(\mathbf{r}_0) + \chi_{ES}^{Byy} \nabla_t E_y^B(\mathbf{r}_0) \right]
 \end{aligned} \tag{1}$$

for the jump in the tangential E -field and

$$\begin{aligned} \mathbf{a}_y \times [\mathbf{E}^A(\mathbf{r}_0) + \mathbf{E}^B(\mathbf{r}_0)] = & -\mathbf{a}_x j\omega\mu_0 [\pi_{MS}^{Axx} H_x^A(\mathbf{r}_0) - \pi_{MS}^{Bxx} H_x^B(\mathbf{r}_0) + \pi_{MS}^{Azz} H_z^A(\mathbf{r}_0) - \pi_{MS}^{Bzz} H_z^B(\mathbf{r}_0)] \\ & - \mathbf{a}_z j\omega\mu_0 [\pi_{MS}^{Axx} H_x^A(\mathbf{r}_0) - \pi_{MS}^{Bxx} H_x^B(\mathbf{r}_0) + \pi_{MS}^{Azz} H_z^A(\mathbf{r}_0) - \pi_{MS}^{Bzz} H_z^B(\mathbf{r}_0)] \\ & - \mathbf{a}_y \times [\pi_{ES}^{Ayy} \nabla_t E_y^A(\mathbf{r}_0) - \pi_{ES}^{Byy} \nabla_t E_y^B(\mathbf{r}_0)] \end{aligned} \quad (2)$$

for the sum (twice the average) of the tangential E -field. The superscripts A and B correspond to the fields in regions A and B (which in general could contain different materials) and \mathbf{r}_0 is a point in the plane $y = 0$ (see Fig. 2). In these expressions, surface parameters χ_{MS} and χ_{ES} are interpreted as effective electric and magnetic surface susceptibilities of the metascreen, and the surface parameters π_{ES} and π_{MS} are interpreted as effective electric and magnetic surface porosities of the metascreen. The subscripts and superscripts in these parameters have the following meanings (see Ref. 4 for details). In their most general form, the surface parameters are different for the fields on either side of the metascreen (indicated by the superscripts “ A ” and “ B ”), where the difference in the surface parameters on either side of the screen is mostly because the materials on either side of the metascreen can be different. The second superscript corresponds to the x , y , or z component of the surface parameters, and the third superscript corresponds to the field component that is associated with the surface parameter. The subscript (ES or MS) indicates whether it is an electric or a magnetic surface parameter. The effective electric and magnetic surface porosities and surface magnetic susceptibilities that appear explicitly in the GSTCs are uniquely defined and, as such, represent the physical quantities that uniquely characterize the metascreen. These GSTCs, along with Maxwell’s equations, are all that are needed to determine macroscopic scattering, transmission, and reflection from the metascreen.

If an electromagnetic wave of a particular polarization is incident onto a surface, and that surface exhibits some type of asymmetry, the reflected and transmitted waves can exhibit other polarizations than that of the incident wave. This is the phenomenon of polarization conversion. Over the years, frequency selective surfaces (FSS), and more recently metasurfaces, have been used to achieve polarization conversion.^{9–20} Most of the metasurface work has been limited to metafilm-type structures. In this paper, we discuss how metascreen-type structures can be used to perform polarization conversion and show how the various surface parameters give rise to these effects.

The magnetic surface parameters in the GSTCs for metascreen can have cross-polarization terms (or off-diagonal terms if written in terms of a dyadic), i.e., $\pi_{MS}^{(A,B)xz}$, $\pi_{MS}^{(A,B)zx}$, $\chi_{MS}^{(A,B)xz}$, and $\chi_{MS}^{(A,B)zx}$. These cross-polarization terms result in coupling (or polarization conversion) between transverse electric (TE) and transverse magnetic (TM) fields (i.e., TE polarized fields will generate TM fields and vice-versa). In this paper, we use the GSTCs to derive the reflection (R) and transmission (T) coefficients for a metascreen composed of anisotropic apertures, and we will illustrate the coupling between TE and TM polarizations.

The derivation presented in Ref. 4 laid out the framework for calculating the required surface susceptibilities and surface

porosities, which require the solution of a set of static field problems—this can be computationally challenging for generally shaped apertures. We will also derive expressions allowing the surface parameters to be retrieved from measured or simulated values of R and T . This is analogous to the modified Nicolson-Ross-Weir (NRW) approach used for retrieving the effective permeability and permittivity of a metamaterial^{21–27} and to the method used to retrieve the surface susceptibilities for a metafilm.^{6,7} Retrieval expressions for isotropic metascreens were derived in Ref. 28; here, we will derive a retrieval approach applicable to the more general case of an anisotropic metascreen. We show that under certain conditions, the expressions presented here for the anisotropic case reduce to the special case of an isotropic metascreen presented in Ref. 28. Finally, we illustrate the use of this retrieval approach by showing results for an anisotropic metascreen composed of an array of asymmetric apertures filled with a high-contrast dielectric.

These GSTCs are valid only under certain conditions. The thickness h of the screen in which the apertures of the metascreen are located is not necessarily zero (or even small compared with the lattice constants). The apertures can be arbitrarily shaped, but their dimensions as well as the screen thickness are required to be sufficiently small in comparison with a wavelength in the surrounding medium (in other words, electrically small). Thus, the expressions for reflection and transmission coefficients, and the retrieval expressions based on them, are only valid with these same restrictions. After we have presented numerical results and compared them with full-wave simulations, we will be able to state these restrictions in a more quantitative manner (see Sec. V).

II. REFLECTION AND TRANSMISSION COEFFICIENTS FOR AN OBLIQUELY INCIDENT PLANE WAVE ONTO A METASCREEN

In this paper, we will assume that the apertures are symmetric about the y -axis and that the material properties in region A and region B are the same. These two assumptions correspond to a large number of the metascreens encountered in practice and result in

$$\begin{aligned} \pi_{MS}^{Axx} = \pi_{MS}^{Bxx} = \pi_{MS}^{xx} \quad \text{and} \quad \pi_{MS}^{Azz} = \pi_{MS}^{Bzz} = \pi_{MS}^{zz}, \\ \chi_{MS}^{Axx} = \chi_{MS}^{Bxx} = \chi_{MS}^{xx} \quad \text{and} \quad \chi_{MS}^{Azz} = \chi_{MS}^{Bzz} = \chi_{MS}^{zz}, \\ \pi_{ES}^{Ayy} = \pi_{ES}^{Byy} = \pi_{ES}^{yy} \quad \text{and} \quad \chi_{ES}^{Ayy} = \chi_{ES}^{Byy} = \chi_{ES}^{yy}, \\ \pi_{MS}^{Axx} = \pi_{MS}^{Bxx} = \pi_{MS}^{xx} \quad \text{and} \quad \chi_{MS}^{Axx} = \chi_{MS}^{Bxx} = \chi_{MS}^{xx}, \\ \pi_{MS}^{Azz} = \pi_{MS}^{Bzz} = \pi_{MS}^{zz} \quad \text{and} \quad \chi_{MS}^{Azz} = \chi_{MS}^{Bzz} = \chi_{MS}^{zz}. \end{aligned} \quad (3)$$

Under these conditions, the GSTCs reduce to a simpler form

$$\begin{aligned} \mathbf{a}_y \times [\mathbf{E}^A(\mathbf{r}_0) - \mathbf{E}^B(\mathbf{r}_0)] &= -\mathbf{a}_x j\omega\mu_0 \{ \chi_{MS}^{xx} [H_x^A(\mathbf{r}_0) + H_x^B(\mathbf{r}_0)] + \chi_{MS}^{xz} [H_z^A(\mathbf{r}_0) + H_z^B(\mathbf{r}_0)] \} \\ &\quad - \mathbf{a}_z j\omega\mu_0 \{ \chi_{MS}^{zz} [H_z^A(\mathbf{r}_0) + H_z^B(\mathbf{r}_0)] + \chi_{MS}^{zx} [H_x^A(\mathbf{r}_0) + H_x^B(\mathbf{r}_0)] \} - \mathbf{a}_y \times \chi_{ES}^{yy} [\nabla_t E_y^A(\mathbf{r}_0) + \nabla_t E_y^B(\mathbf{r}_0)] \end{aligned} \quad (4)$$

and

$$\begin{aligned} \mathbf{a}_y \times [\mathbf{E}^A(\mathbf{r}_0) + \mathbf{E}^B(\mathbf{r}_0)] &= -\mathbf{a}_x j\omega\mu_0 \{ \pi_{MS}^{xx} [H_x^A(\mathbf{r}_0) - H_x^B(\mathbf{r}_0)] + \pi_{MS}^{xz} [H_z^A(\mathbf{r}_0) - H_z^B(\mathbf{r}_0)] \} \\ &\quad - \mathbf{a}_z j\omega\mu_0 \{ \pi_{MS}^{zz} [H_z^A(\mathbf{r}_0) - H_z^B(\mathbf{r}_0)] + \pi_{MS}^{zx} [H_x^A(\mathbf{r}_0) - H_x^B(\mathbf{r}_0)] \} - \mathbf{a}_y \times \pi_{ES}^{yy} [\nabla_t E_y^A(\mathbf{r}_0) - \nabla_t E_y^B(\mathbf{r}_0)]. \end{aligned} \quad (5)$$

A. TE polarization

Let a metascreen be centered on the plane $y = 0$ in free space. Assume that a TE-polarized plane wave is incident at an angle θ onto the metascreen shown in Fig. 3(a) such that the incident field is given by

$$\mathbf{E}^i = \mathbf{a}_z E_0 e^{-j\mathbf{k}_i \cdot \mathbf{r}}, \quad (6)$$

where

$$\mathbf{k}_i = \{ \mathbf{a}_x \sin \theta - \mathbf{a}_y \cos \theta \} k_0. \quad (7)$$

To account for the possibility of the metascreen converting the incident TE wave into both TE and TM waves [see Fig. 3(a)], the reflected and transmitted field are expressed as

$$\mathbf{E}^r = \mathbf{a}_z R_{TE} E_0 e^{-j\mathbf{k}_r \cdot \mathbf{r}} + R_{TE}^{TM} E_0 (\mathbf{a}_x \cos \theta - \mathbf{a}_y \sin \theta) e^{-j\mathbf{k}_r \cdot \mathbf{r}} \quad (8)$$

and

$$\mathbf{E}^t = \mathbf{a}_z T_{TE} E_0 e^{-j\mathbf{k}_t \cdot \mathbf{r}} + T_{TE}^{TM} E_0 (\mathbf{a}_x \cos \theta + \mathbf{a}_y \sin \theta) e^{-j\mathbf{k}_t \cdot \mathbf{r}}, \quad (9)$$

where

$$\mathbf{k}_t = \mathbf{k}_i \quad \text{and} \quad \mathbf{k}_r = \{ \mathbf{a}_x \sin \theta + \mathbf{a}_y \cos \theta \} k_0, \quad (10)$$

and R_{TE} and T_{TE} are the reflection and transmission coefficients of a TE wave, and R_{TE}^{TM} and T_{TE}^{TM} are the reflection and transmission coefficients of a TM wave for an incident TE wave. If the cross-coupling terms (χ_{MS}^{xz} and π_{MS}^{zx}) are zero, then R_{TE}^{TM} and T_{TE}^{TM} should be zero and we are left with a pure TE reflection and transmitted field.

Using Maxwell's equations, the incident, reflected, and transmitted H-fields become

$$\mathbf{H}^i = \frac{E_0}{\eta} (-\mathbf{a}_x \cos \theta - \mathbf{a}_y \sin \theta) e^{-j\mathbf{k}_i \cdot \mathbf{r}}, \quad (11)$$

$$\mathbf{H}^r = R_{TE} \frac{E_0}{\eta} (\mathbf{a}_x \cos \theta - \mathbf{a}_y \sin \theta) e^{-j\mathbf{k}_r \cdot \mathbf{r}} - \mathbf{a}_z R_{TE}^{TM} \frac{E_0}{\eta} e^{-j\mathbf{k}_r \cdot \mathbf{r}}, \quad (12)$$

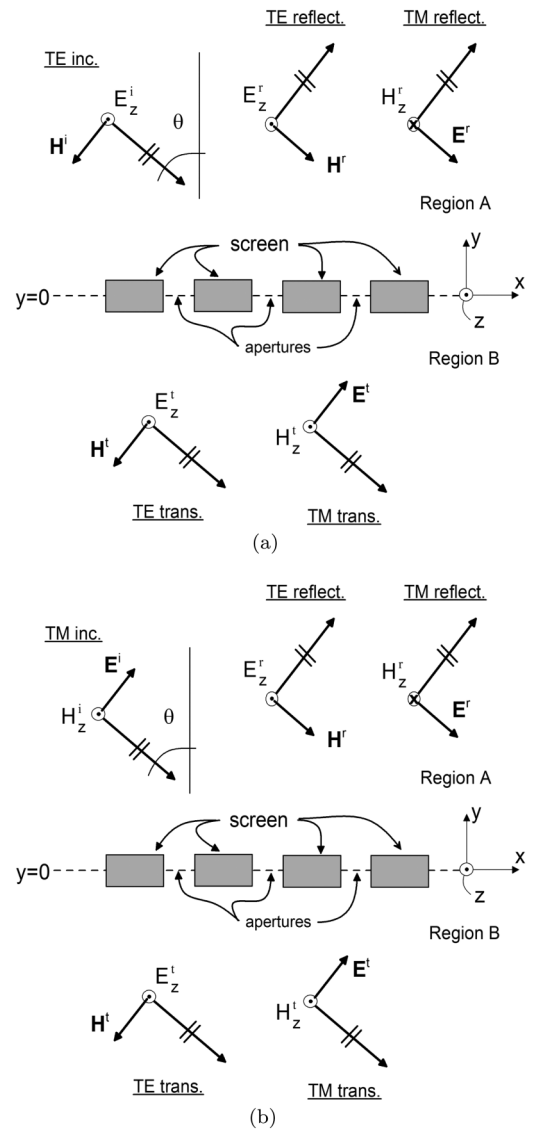


FIG. 3. Plane wave incident onto a metascreen: (a) TE polarization and (b) TM polarization.

and

$$\mathbf{H}^t = -T_{TE} \frac{E_0}{\eta} (\mathbf{a}_x \cos \theta + \mathbf{a}_y \sin \theta) e^{-j\mathbf{k}_i \cdot \mathbf{r}} + \mathbf{a}_z T_{TE}^{TM} \frac{E_0}{\eta} e^{-j\mathbf{k}_i \cdot \mathbf{r}}, \quad (13)$$

where $\eta = \sqrt{\mu/\epsilon}$ is the intrinsic impedance of free space.

Substituting the electric and magnetic field components given in Eqs. (6)–(13), into the GSTCs given in Eqs. (4) and (5), we obtain the following reflection and transmission coefficients:

$$R_{TE}(\theta) = 1 - \frac{A}{X(A + \frac{V}{4X})} - \frac{B}{Y(B + \frac{4W}{Y})}, \quad (14)$$

$$T_{TE}(\theta) = -\frac{\frac{1}{4} \frac{V}{X}}{X(A + \frac{V}{4X})} + \frac{\frac{4}{Y} \frac{W}{Y}}{Y(B + \frac{4W}{Y})} + \frac{j2k_0 \pi_{MS}^{xx} \cos \theta}{Y} - \frac{j \frac{k_0}{2} \chi_{MS}^{xx} \cos \theta}{X}, \quad (15)$$

$$R_{TE}^{TM}(\theta) = -\frac{j \frac{k_0}{2} \chi_{MS}^{zx} \cos \theta}{X(A + \frac{V}{4X})} - \frac{j2k_0 \pi_{MS}^{zx} \cos \theta}{Y(B + \frac{4W}{Y})}, \quad (16)$$

and

$$T_{TE}^{TM}(\theta) = \frac{j \frac{k_0}{2} \chi_{MS}^{zx} \cos \theta}{X(A + \frac{V}{4X})} - \frac{j2k_0 \pi_{MS}^{zx} \cos \theta}{Y(B + \frac{4W}{Y})}, \quad (17)$$

where

$$A = \cos \theta + j \frac{k_0}{2} \chi_{MS}^{zz} + j \frac{k_0}{2} \chi_{ES}^{yy} \sin^2 \theta, \quad (18)$$

$$B = \cos \theta + j2k_0 \pi_{MS}^{zz} + j2k_0 \pi_{ES}^{yy} \sin^2 \theta, \quad (19)$$

$$X = 1 + j \frac{k_0}{2} \chi_{MS}^{xx} \cos \theta, \quad Y = 1 + j2k_0 \pi_{MS}^{xx} \cos \theta, \quad (20)$$

$$V = k_0^2 \chi_{MS}^{xz} \chi_{MS}^{zx} \cos \theta, \quad W = k_0^2 \pi_{MS}^{xz} \pi_{MS}^{zx} \cos \theta. \quad (21)$$

From these expressions, we see that due to the anisotropic terms in the GSTC (χ_{MS}^{xz} and π_{MS}^{zx}), polarization conversion will occur, in that an incident TE wave will generate a TM wave. If the anisotropic terms are zero (i.e., $\chi_{MS}^{xz} = 0$, $\pi_{MS}^{zx} = 0$), then $R_{TE}^{TM} = 0$ and $T_{TE}^{TM} = 0$, and R_{TE} and T_{TE} reduce to Eqs. (12) and (13) given in Ref. 28. In this case, we are left with a pure TE reflected and transmitted field.²⁸

B. TM polarization

Assume that a TM-polarized plane wave is incident onto the metascreen shown in Fig. 3(b) such that the incident fields are given by

$$\mathbf{E}^i = E_0 (\mathbf{a}_x \cos \theta + \mathbf{a}_y \sin \theta) e^{-j\mathbf{k}_i \cdot \mathbf{r}}. \quad (22)$$

As above, to account for the possibility of the metascreen converting the incident TM wave into both TE and TM waves [see Fig. 3(b)], the reflected and transmitted fields are expressed as

$$\mathbf{E}^r = \mathbf{a}_z R_{TM}^{TE} E_0 e^{-j\mathbf{k}_r \cdot \mathbf{r}} + R_{TM} E_0 (\mathbf{a}_x \cos \theta - \mathbf{a}_y \sin \theta) e^{-j\mathbf{k}_r \cdot \mathbf{r}} \quad (23)$$

and

$$\mathbf{E}^t = \mathbf{a}_z T_{TM}^{TE} E_0 e^{-j\mathbf{k}_t \cdot \mathbf{r}} + T_{TM} E_0 (\mathbf{a}_x \cos \theta + \mathbf{a}_y \sin \theta) e^{-j\mathbf{k}_t \cdot \mathbf{r}}, \quad (24)$$

where R_{TM} and T_{TM} are the reflection and transmission coefficients of the TM wave and R_{TM}^{TE} and T_{TM}^{TE} are the reflection and transmission coefficients of a TE wave for an incident TM wave. If the cross-coupling terms (χ_{MS}^{xz} and π_{MS}^{zx}) are zero, then R_{TM}^{TE} and T_{TM}^{TE} would be zero and we are left with a pure TM reflection and transmitted field.

From Maxwell's equations, the incident, reflected, and transmitted H-fields become

$$\mathbf{H}^i = \mathbf{a}_z \frac{E_0}{\xi} e^{-j\mathbf{k}_i \cdot \mathbf{r}}, \quad (25)$$

$$\mathbf{H}^r = R_{TM}^{TE} \frac{E_0}{\eta} (\mathbf{a}_x \cos \theta - \mathbf{a}_y \sin \theta) e^{-j\mathbf{k}_r \cdot \mathbf{r}} - \mathbf{a}_z R_{TM} \frac{E_0}{\eta} e^{-j\mathbf{k}_r \cdot \mathbf{r}}, \quad (26)$$

and

$$\mathbf{H}^t = -T_{TM}^{TE} \frac{E_0}{\eta} (\mathbf{a}_x \cos \theta + \mathbf{a}_y \sin \theta) e^{-j\mathbf{k}_t \cdot \mathbf{r}} + \mathbf{a}_z T_{TM} \frac{E_0}{\eta} e^{-j\mathbf{k}_t \cdot \mathbf{r}}. \quad (27)$$

Substituting the electric and magnetic field components given in Eqs. (22)–(27), into the GSTCs given in Eqs. (4) and (5), we obtain the following:

$$R_{TM}(\theta) = 1 - \frac{\cos \theta}{A + \frac{V}{4X}} - \frac{\cos \theta}{B + \frac{4W}{Y}}, \quad (28)$$

$$T_{TM}(\theta) = \frac{\cos \theta}{A + \frac{V}{4X}} - \frac{\cos \theta}{B + \frac{4W}{Y}}, \quad (29)$$

$$R_{TM}^{TE}(\theta) = -\frac{j \frac{k_0}{2} \chi_{MS}^{xz} \cos \theta}{X[A + \frac{V}{4X}]} - \frac{j2k_0 \pi_{MS}^{xz} \cos \theta}{Y[B + \frac{4W}{Y}]}, \quad (30)$$

and

$$T_{TM}^{TE}(\theta) = \frac{j \frac{k_0}{2} \chi_{MS}^{xz} \cos \theta}{X[A + \frac{V}{4X}]} - \frac{j2k_0 \pi_{MS}^{xz} \cos \theta}{Y[B + \frac{4W}{Y}]}. \quad (31)$$

From these expressions, we see that due to the anisotropic terms in the GSTC (χ_{MS}^{xz} and π_{MS}^{zx}), polarization conversion will occur in

that an incident TM wave will generate a TE wave. If the anisotropic terms are zero (i.e., $\chi_{MS}^{xz,zx} = 0$ and $\pi_{MS}^{xz,zx} = 0$), then $R_{TM}^{TE} = 0$ and $T_{TM}^{TE} = 0$, and R_{TM} and T_{TM} reduce to Eqs. (16) and (17) given in Ref. 28. In this case, we are left with a pure TM reflected and transmitted field.²⁸

These types of polarization-conversion reflection and transmission coefficients have been derived for anisotropic metafilms by Saleh *et al.*^{29,30} Similar to what we have shown for an anisotropic metascreen, they found that the polarization-conversion coefficients become zero for an isotropic metafilm and their results reduce to the pure TE or pure TM cases given in Refs. 1, 6, and 7.

III. RETRIEVAL ALGORITHMS FOR THE SURFACE PARAMETERS

It is useful to be able to determine the surface parameters that characterize a metascreen by a method other than direct numerical computation as discussed in Ref. 4. Such a retrieval approach for metafilms is presented in Refs. 1, 6, and 7. Here, we derive a retrieval approach applicable to the more general case of an anisotropic metascreen. Such a method applicable to isotropic metascreens is given in Ref. 28.

From Eqs. (14)–(17) and (28)–(31), we see that there are eight equations (for R_{TE} , T_{TE} , R_{TE}^{TM} , T_{TE}^{TM} , R_{TM} , T_{TM} , R_{TM}^{TE} , and T_{TM}^{TE}) and ten unknowns (χ_{MS}^{xx} , χ_{MS}^{yy} , χ_{MS}^{zz} , χ_{MS}^{xz} , χ_{MS}^{zx} , π_{MS}^{xx} , π_{MS}^{yy} , π_{MS}^{zz} , and π_{MS}^{xz}). Since these eight equations are valid for any angle, we first set $\theta = 0$. This essentially eliminates two of the unknowns, i.e., χ_{ES}^{yy} and π_{ES}^{yy} . We now have eight equations and eight unknowns that can be solved to give

$$\chi_{MS}^{zz} = \frac{2 \Delta_1^+}{jk_0 \Delta_3^-}; \quad \pi_{MS}^{zz} = \frac{-1 \Delta_2^+}{2jk_0 \Delta_3^+}, \quad (32)$$

$$\chi_{MS}^{xx} = \frac{2 \Delta_1^-}{jk_0 \Delta_3^-}; \quad \pi_{MS}^{xx} = \frac{-1 \Delta_2^-}{2jk_0 \Delta_3^+}, \quad (33)$$

$$\chi_{MS}^{xz} = \frac{4 [T_{TM}^{TE}(0) - R_{TM}^{TE}(0)]}{jk_0 \Delta_3^-}, \quad (34)$$

$$\chi_{MS}^{zx} = \frac{4 [T_{TE}^{TM}(0) - R_{TE}^{TM}(0)]}{jk_0 \Delta_3^-}, \quad (35)$$

$$\pi_{MS}^{xz} = \frac{1 [T_{TM}^{TE}(0) + R_{TM}^{TE}(0)]}{jk_0 \Delta_3^+}, \quad (36)$$

$$\pi_{MS}^{zx} = \frac{1 [T_{TE}^{TM}(0) + R_{TE}^{TM}(0)]}{jk_0 \Delta_3^+}, \quad (37)$$

where

$$\Delta_1^\pm = [1 \pm T_{TE}(0) \mp R_{TE}(0)][1 \pm R_{TM}(0) \mp T_{TM}(0)] + [R_{TE}^{TM}(0) - T_{TE}^{TM}(0)][R_{TM}^{TE}(0) - T_{TM}^{TE}(0)], \quad (38)$$

$$\Delta_2^\pm = [1 \pm T_{TE}(0) \pm R_{TE}(0)][1 \mp R_{TM}(0) \mp T_{TM}(0)] + [R_{TE}^{TM}(0) + T_{TE}^{TM}(0)][R_{TM}^{TE}(0) + T_{TM}^{TE}(0)], \quad (39)$$

$$\Delta_3^\pm = [T_{TE}(0) \pm R_{TE}(0) \mp 1][1 - R_{TM}(0) \mp T_{TM}(0)] + [R_{TE}^{TM}(0) \pm T_{TE}^{TM}(0)][R_{TM}^{TE}(0) \pm T_{TM}^{TE}(0)]. \quad (40)$$

Using reflection and transmission coefficient data for some suitable $\theta \neq 0$, we can now compute the two remaining surface parameters. To determine π_{ES}^{yy} , we add Eqs. (28) and (29) to obtain

$$B = \frac{2 \cos \theta}{1 - T_{TM}(\theta) - R_{TM}(\theta)} - \frac{4W}{Y}, \quad (41)$$

and once this is substituted into (19), we obtain

$$\pi_{ES}^{yy}(\theta) = \frac{1}{2jk_0 \sin^2 \theta} \left[\frac{2 \cos \theta}{1 - T_{TM}(\theta) - R_{TM}(\theta)} - \frac{4W}{Y} - j2k_0 \pi_{MS}^{zz} - \cos \theta \right]. \quad (42)$$

Similarly, for χ_{ES}^{yy} , we subtract (28) and (29) to obtain

$$A = \frac{2 \cos \theta}{1 + T_{TM}(\theta) - R_{TM}(\theta)} - \frac{V}{4X}, \quad (43)$$

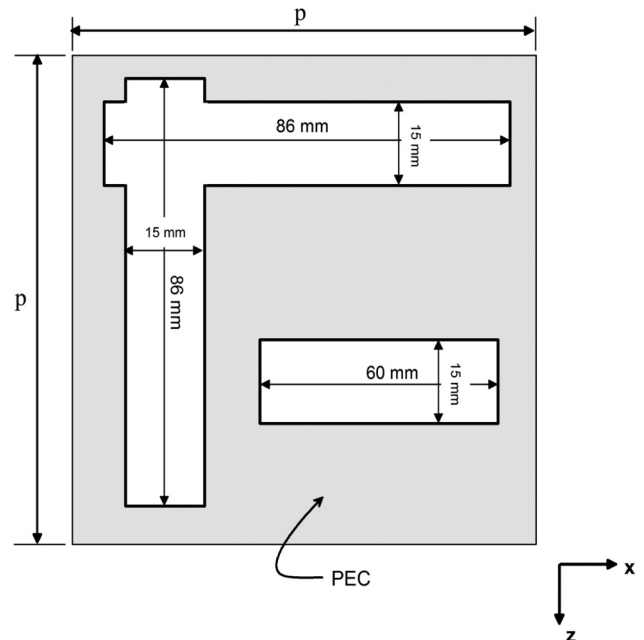
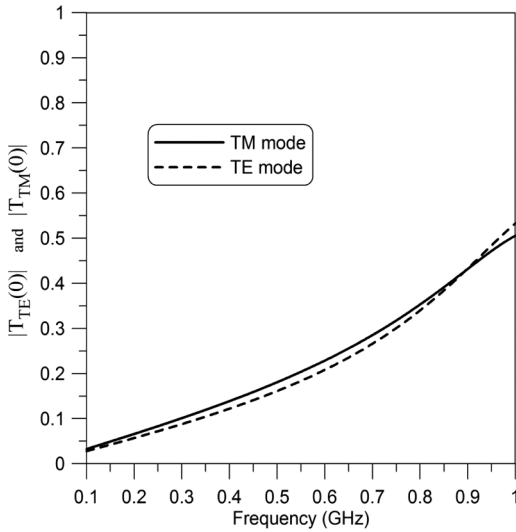


FIG. 4. Period cell of the asymmetric aperture that composes the metascreen with $p = 100$ mm and a screen thickness of $h = 5$ mm.

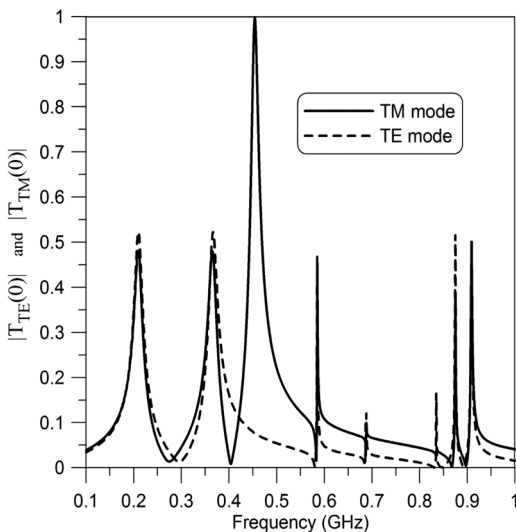
and once this is substituted into (18), we obtain

$$\chi_{ES}^{yy} = \frac{2}{jk_0 \sin^2 \theta} \left[\frac{2 \cos \theta}{1 + T_{TM}(\theta) - R_{TM}(\theta)} - \frac{V}{4X} - j \frac{k_0}{2} \chi_{MS}^{zz} - \cos \theta \right]. \quad (44)$$

For an isotropic metascreen, the cross-coupling surface parameters ($\chi_{MS}^{xz, zx}$ and $\pi_{MS}^{xz, zx}$) are zero, and thus, R_{TE}^{TM} , T_{TE}^{TM} , R_{TM}^{TE} , and T_{TM}^{TE} are



(a)



(b)

FIG. 5. HFSS numerical values for the transmission coefficient: (a) no material filling and (b) material filling for a metascreen composed of the asymmetric apertures shown in Fig. 4. The material filling corresponds to $\epsilon_r = 108.2$ and $\tan \delta = 4.9 \times 10^{-5}$.

also zero. It can be shown that under these conditions, Eqs. (32)–(37), (42), and (44) reduce to the retrieval expressions for an isotropic metascreen given in Ref. 28.

IV. TRANSMISSION THROUGH A METASCREEN FILLED WITH A HIGH-CONTRAST DIELECTRIC

When designing metascreens by tailoring the surface parameters (i.e., surface susceptibilities and porosities), interesting and unique reflection and transmission properties of the metascreen can be achieved. An in-depth investigation will be the topic of a future publication. However, to briefly illustrate some of the interesting properties, we will discuss one example here. Consider a metascreen composed of the array of asymmetric apertures depicted in Fig. 4, with the screen being a perfect electric conductor (PEC). We consider two cases: (1) the aperture is filled with free-space and (2) the aperture is filled with a high-contrast dielectric with $\epsilon_r = 108.2$ and a loss tangent of $\tan \delta = 4.9 \times 10^{-5}$ (these material properties actually represent a commercially available material).

The transmission coefficients for this metascreen (for normal incidence) are determined numerically from the full-wave finite-element software HFSS (mentioning this product does not imply an endorsement, but it serves to clarify the numerical program used). Figure 5 shows the magnitude of T_{TE} and T_{TM} for the cases with and without material filling at $\theta = 0^\circ$. Note that TE corresponds to the E-field polarization in the z -direction as indicated by the aperture geometry shown in Fig. 4. It is interesting to observe that when no material filling is used, the transmission properties for both TE and TM cases exhibit a very similar behavior [see Fig. 5(a)], where both show a monotonic increase from low frequency and both show a maximum transmission of 50% at 1 GHz. However, when the aperture is filled with the high-contrast dielectric, the two polarizations behave differently from one

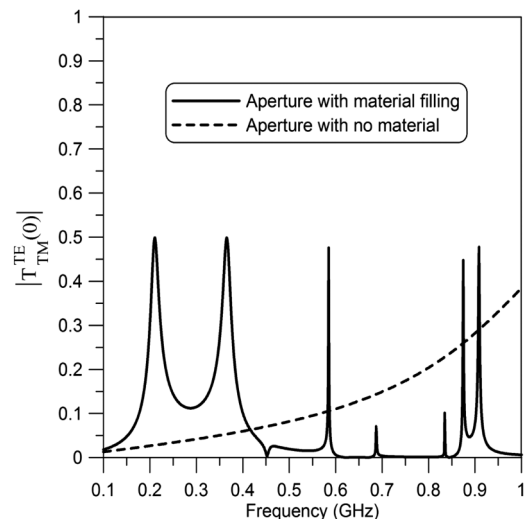


FIG. 6. HFSS numerical values for the transmission coefficient for a metascreen of Fig. 4: comparison of $|T_{TM}^{TE}|$ with and without material fillings.

another. In particular, the *TM* polarization achieves 100% transmission at 0.5 GHz. From Fig. 5, we see that besides the instance of 100% transmission, there are other frequencies where sharp resonances occur (these resonances are not present when no filling is used). While we do see sharp resonances for the *TE* case, we do not see the 100% transmission that was observed for the *TM* case.

Figure 6 shows the polarization conversion from *TM* to *TE* for the cases with and without the high-contrast dielectric filling. We see that the high-contrast dielectric causes about 50% polarization conversion from the *TM* to *TE* at frequencies as low as 0.2 GHz and exhibits sharp resonances across the entire frequency band (again, these resonances are not present when no filling is used).

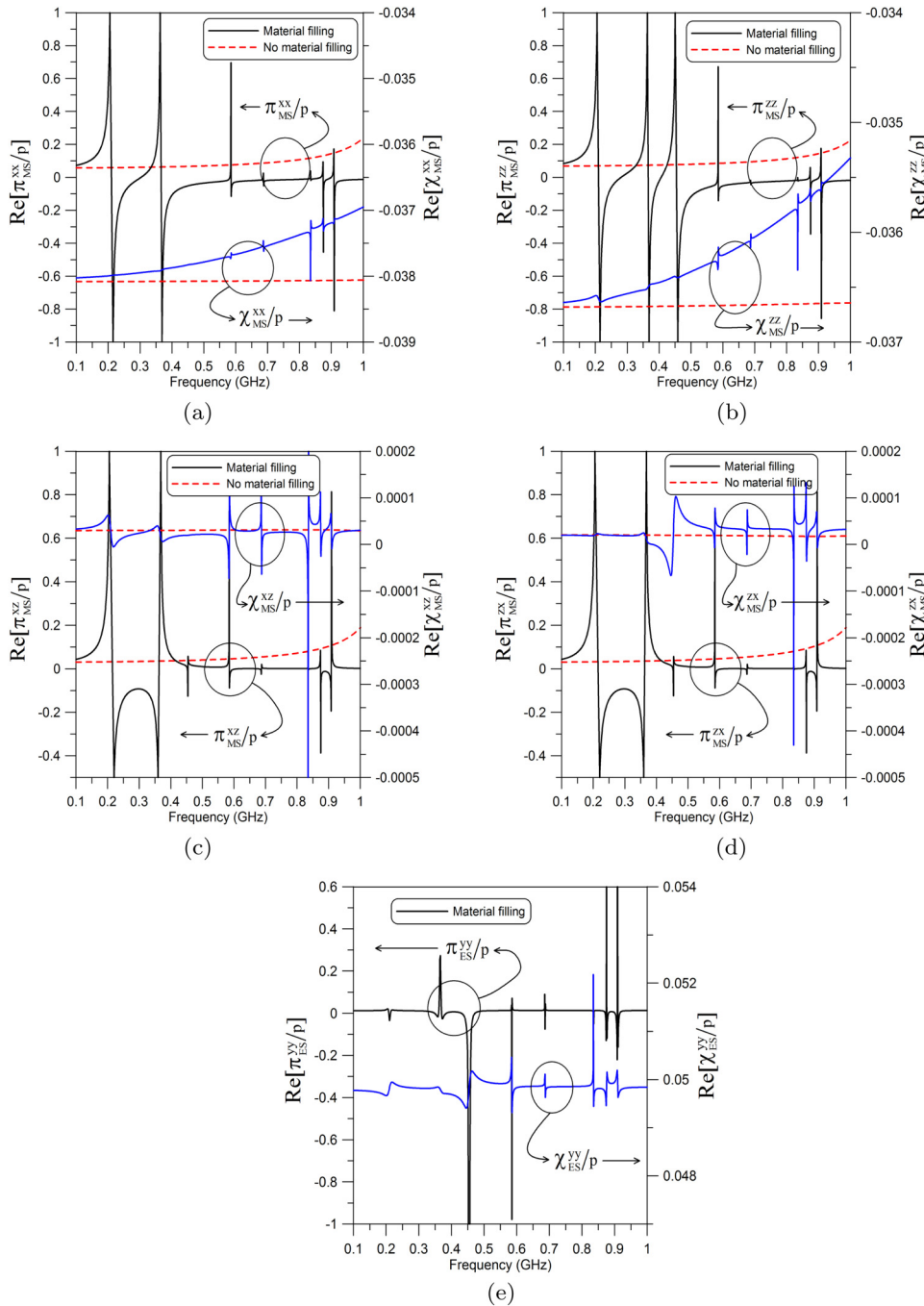


FIG. 7. Retrieved surface parameters for an array of asymmetric apertures with and without a high-contrast material for $h = 5$ mm and $p = 100$ mm: (a) π_{MS}^{xx} and χ_{MS}^{xx} , (b) π_{MS}^{zz} and χ_{MS}^{zz} , (c) π_{MS}^{xz} and χ_{MS}^{xz} , (d) π_{MS}^{zx} and χ_{MS}^{zx} , and (e) π_{ES}^{yy} and χ_{MS}^{yy} .

used). In principle, it should be possible to design the aperture geometry (and material filling) in order to achieve 100% mode conversion over a narrow frequency range. We see that the use of high-contrast dielectrics can lead to the possibility of designing metascreens with unique transmission and reflection properties (e.g., narrow band filters as well as other applications).

Using the HFSS results for $R_{TE}(0)$, $T_{TE}(0)$, $R_{TM}(0)$, $T_{TM}(0)$, $R_{TE}^{TM}(0)$, $T_{TE}^{TM}(0)$, $R_{TM}^{TE}(0)$, and $T_{TM}^{TE}(0)$ for this anisotropic metascreen, we used Eqs. (32)–(37) to determine the surface parameters (i.e., $\pi_{MS}^{xx,zz}$, $\chi_{MS}^{xx,zz}$, $\pi_{MS}^{xz,xz}$, $\chi_{MS}^{xz,xz}$) for this anisotropic metascreen. These retrieved values are shown in Fig. 7. We used HFSS results

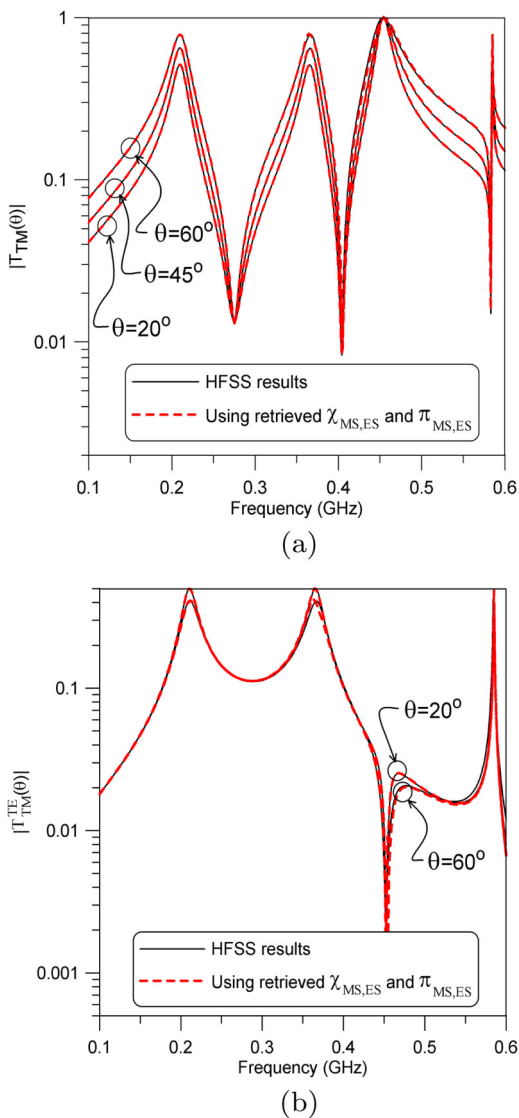


FIG. 8. Comparison of transmission coefficients for 20° , 45° , and 60° for an array of apertures filled with a high-contrast material ($\epsilon_r = 108.2$ and $\tan \delta = 4.9 \times 10^{-5}$): (a) $|T_{TM}(\theta)|$ and (b) $|T_{TM}^{TE}(\theta)|$.

for $R_{TM}(30^\circ)$ and $T_{TM}(30^\circ)$ along with Eqs. (42) and (44) to determine π_{ES}^{yy} and χ_{ES}^{yy} . These two surface parameters are also shown in Fig. 7. Shown here are the surface parameters with and without the high-contrast materials inside the apertures. We see from these plots that resonances in the surface parameters are present when the apertures are filled with the high-permittivity material, while no such resonance is present in this frequency range without the material filling present. We see that in general, the amplitudes of the resonances in $\pi_{MS,ES}$ are about an order of magnitude larger than those seen in $\chi_{MS,ES}$. It is interesting to observe which of the surface parameters give rise to the various resonances seen in the transmission coefficients. For example, there is a resonance in $|T_{TM}(0)|$ at 0.45 GHz, while there is no resonance in $|T_{TE}(0)|$ at that same frequency. The resonance in π_{MS}^{zz} at 0.45 GHz [see Fig. 7(b)] appears to be what gives rise to the resonance in $|T_{TM}|$. Note that no resonance is seen in π_{MS}^{xx} at 0.45 GHz.

Using the retrieved values for the surface parameters, along with Eqs. (14)–(17) and (28)–(31), the reflection and transmission coefficients for various other angles of incidence can be determined. The values for $T_{TM}(\theta)$ and $T_{TM}^{TE}(\theta)$ are calculated from (29) and (31), and using the results given in Fig. 7 are shown in Fig. 8, for 20° , 45° , and 60° . For a comparison, also in this figure, we show full-wave numerical results obtained from HFSS. These comparisons show that the transmission coefficients obtained from the surface parameters are indistinguishable from the HFSS results, even for angles as high as 60° . Thus, the retrieved parameters are not sensitive to the incidence angles used to determine them.

V. DISCUSSION AND CONCLUSION

Electromagnetic field interactions with a metascreen are best characterized by generalized sheet-transition conditions (GSTCs). The surface parameters (the effective electric and magnetic surface susceptibilities and surface porosities) that appear explicitly in the GSTCs are uniquely defined and as such serve as the physical quantities that most appropriately characterize the metascreen. These effective surface parameters for any given metascreen, together with the GSTCs given in Eqs. (1) and (2), are all that are required to model its interaction with an EM field. We used the GSTCs to derive the reflection and transmission coefficients for a metascreen composed of an array of anisotropic apertures, expressed in terms of the electric and magnetic surface parameters (the effective electric and magnetic surface susceptibilities and surface porosities). The results here illustrate that the cross-polarization surface parameters result in coupling (or polarization conversion) between TE and TM waves when a plane wave is incident onto a metascreen. We showed an example of such polarization conversion and illustrate the unique behavior of a metascreen when a high-contrast dielectric fills the apertures. In fact, by tailoring the surface parameters (i.e., surface susceptibilities and porosities) by either geometry and/or material filling, it is possible to design metascreens with unique reflection and transmission properties (e.g., narrow band filters as well as other applications). More importantly, it is possible to design surfaces that would have unique polarization conversion properties, achieving 100% polarization conversion over a narrow frequency range.

We have used the expressions for the reflection and transmission coefficients obtained here to derive a retrieval approach for

determining all the surface parameters needed to characterize an anisotropic metascreen. This retrieval approach was demonstrated by showing results for an anisotropic metascreen composed of an array of asymmetric apertures filled with a high-contrast dielectric. We show that with these retrieved values for the surface parameters, along with Eqs. (14)–(17) and (28)–(31), the reflection and transmission coefficients for any angle of incidence can be determined. We validated this by showing comparisons for the transmission coefficient obtained from the retrieved surface parameters with those obtained from HFSS full-wave numerical results. The results from these two approaches are graphically indistinguishable, even for angles as high as 60° .

The computed data for the cases examined in Sec. IV suggest that very accurate results can be obtained from the method of this paper as long as the characteristic dimensions of the aperture are less than about 0.33λ . We emphasize that the wavelength in question is that of the external medium and that the aperture itself may contain a high-permittivity material in which the wavelength is comparable to or smaller than the aperture dimensions without degrading the accuracy of the results.

The GSTCs derived in Ref. 4 are applicable for the general case when different materials are on each side of the metascreen. In this paper, we have limited ourselves to the consideration of asymmetric metascreens with identical media on both sides. While this assumption corresponds to a large number of the metascreens encountered in practice, the case of an asymmetric metascreen with different media on the two sides will be the subject of future work.

REFERENCES

- ¹C. L. Holloway, E. F. Kuester, J. A. Gordon, J. O'Hara, J. Booth, and D. R. Smith, "An overview of the theory and applications of metasurfaces: The two-dimensional equivalents of metamaterials," *IEEE Antennas Propag. Mag.* **54** (2), 10–35 (2012).
- ²*Structured Surfaces as Optical Metamaterials*, edited by A. A. Maradudin (Cambridge University Press, Cambridge, UK, 2011).
- ³E. F. Kuester, M. A. Mohamed, M. Piket-May, and C. L. Holloway, "Averaged transition conditions for electromagnetic fields at a metafilm," *IEEE Trans. Antennas Propag.* **51**, 2641–2651 (2003).
- ⁴C. L. Holloway and E. F. Kuester, "Generalized sheet transition conditions (GSTCs) for a metascreen," *IEEE Trans. Antennas Propag.* **66**, 2414–2427 (2018).
- ⁵C. L. Holloway, E. F. Kuester, and A. Dienstfrey, "A homogenization technique for obtaining generalized sheet transition conditions for an arbitrarily shaped coated-wire grating," *Radio Sci.* **49**, 813–850 (2014).
- ⁶C. L. Holloway, A. Dienstfrey, E. F. Kuester, J. F. O'Hara, A. K. Azad, and A. J. Taylor, "A discussion on the interpretation and characterization of metafilms-metasurfaces: The two-dimensional equivalent of metamaterials," *Metamaterials* **3**, 100–112 (2009).
- ⁷C. L. Holloway, E. F. Kuester, and A. Dienstfrey, "Characterizing metasurfaces/metafilms: The connection between surface susceptibilities and effective material properties," *IEEE Ant. Wireless Prop. Lett.* **10**, 1507–1511 (2011).
- ⁸C. L. Holloway and E. F. Kuester, "A homogenization technique for obtaining generalized sheet transition conditions (GSTCs) for a metafilm embedded in a magneto-dielectric interface," *IEEE Trans. Antennas Propag.* **64**, 4671–4686 (2016).
- ⁹A. B. Khanikaev, S. H. Mousavi, C. Wu, N. Dabidian, K. B. Alici, and G. Shvets, "Electromagnetically induced polarization conversion," *Opt. Commun.* **285**, 3423–3427 (2012).
- ¹⁰T. W. H. Oates, B. Dastmalchi, C. Helgert, L. Reissmann, U. Huebner, E.-B. Kley, M. A. Verschuuren, I. Bergmair, T. Pertsch, K. Hingerl, and K. Hinrichs, "Optical activity in sub-wavelength metallic grids and fishnet metamaterials in the conical mount," *Opt. Mater. Express* **3**, 439–451 (2013).
- ¹¹C. Pfeiffer and A. Grbic, "Cascaded metasurfaces for complete phase and polarization control," *Appl. Phys. Lett.* **102**, 231116 (2013).
- ¹²H. L. Zhu, S. W. Cheung, K. L. Chung, and T. I. Yuk, "Linear-to-circular polarization conversion using metasurface," *IEEE Trans. Antennas Propag.* **61**, 4615–4623 (2013).
- ¹³C. Pfeiffer, C. Zhang, V. Ray, L. J. Guo, and A. Grbic, "High performance bianisotropic metasurfaces: Asymmetric transmission of light," *Phys. Rev. Lett.* **113**, 023902 (2014).
- ¹⁴L. Jian-Xing, Z. An-Xue, W. Jia-Fu, and X. Zhuo, "Tri-band transparent cross-polarization converters using a chiral metasurface," *Chin. Phys. B* **23**, 118101 (2014).
- ¹⁵P. Boyer, "Jones matrices of perfectly conducting metallic polarizers," *J. Opt. Soc. Am. A* **31**, 1126–1232 (2014).
- ¹⁶W. Wang, Z. Guo¹, R. Li, J. Zhang, A. Zhang, Y. Li, Y. Liu, X. Wang, and S. Qu, "L-shaped metasurface for both the linear and circular polarization conversions," *J. Opt.* **17**, 065103 (2015).
- ¹⁷N. M. Estakhri and A. Alu, "Wave-front transformation with gradient metasurfaces," *Phys. Rev. X* **6**, 041008 (2016).
- ¹⁸A. Epstein and G. V. Eleftheriades, "Arbitrary power-conserving field transformations with passive lossless omega-type bianisotropic metasurfaces," *IEEE Trans. Antennas Propag.* **64**, 3880–3895 (2017).
- ¹⁹H. Dai, Y. Zhao, H. Sun, J. Chen, Y. Ge, and Z. Li, "An ultra-wideband linear polarization conversion metasurface," *Jpn. J. Appl. Phys.* **57**, 090311 (2018).
- ²⁰Y.-X. Peng, K.-J. Wang, M.-D. He, J. H. Luo, X.-M. Zhang, J.-B. Li, S.-H. Tan, J.-Q. Liu, W.-D. Hu, and X. Chen, "Electromagnetic near-field coupling induced polarization conversion and asymmetric transmission in plasmonic metasurfaces," *Opt. Commun.* **412**, 1–6 (2018).
- ²¹A. M. Nicolson and G. Ross, "Measurement of the intrinsic properties of materials by time domain techniques," *IEEE Trans. Instrum. Meas.* **19**, 377–382 (1970).
- ²²W. B. Weir, "Automatic measurements of complex dielectric constant and permeability at microwave frequencies," *Proc. IEEE* **62**, 33–36 (1974).
- ²³D. R. Smith, S. Schultz, P. Markos, and C. M. Soukoulis, "Determination of effective permittivity and permeability of metamaterials from reflection and transmission coefficients," *Phys. Rev. B* **65**, 195104 (2002).
- ²⁴R. W. Ziolkowski, "Designs, fabrication, and testing of double negative metamaterials," *IEEE Trans. Antennas Propag.* **51**, 1516–1529 (2003).
- ²⁵S. Kim, E. F. Kuester, C. L. Holloway, A. D. Scher, and J. Baker-Jarvis, "Boundary effects on the determination of the effective parameters of a metamaterial from normal incidence reflection and transmission measurements," *IEEE Trans. Antennas Propag.* **59**, 2226–2240 (2011).
- ²⁶S. Kim, E. F. Kuester, C. L. Holloway, A. D. Scher, and J. Baker-Jarvis, "Effective material property extraction of a metamaterial by taking boundary effects into account at TE/TM polarized incidence," *Prog. Electromagn. Res. B* **36**, 1–33 (2011).
- ²⁷X. Chen, T. M. Grzegorzczak, B.-I. Wu, J. Pacheco, and J. A. Kong, "Robust method to retrieve the constitutive effective parameters of metamaterials," *Phys. Rev. E* **70**, 016608 (2004).
- ²⁸C. L. Holloway and E. F. Kuester, "Reflection and transmission coefficients for a metascreen: Retrieval approach for determining effective surface-susceptibilities and surface- porosities," [arXiv:1902.08703v1](https://arxiv.org/abs/1902.08703v1), 22 Feb, 2019.
- ²⁹A. M. Saleh, K. R. Mahmoud, I. I. Ibrahim, and A. M. Attiya, "Analysis of anisotropic metasurfaces using generalized sheet transition condition," *J. Electromagn. Waves Appl.* **30**(5), 661–675 (2016).
- ³⁰A. M. Saleh, K. R. Mahmoud, I. I. Ibrahim, and A. M. Attiya, "Generalized sheet transition condition (GSTC) for anisotropic metasurfaces," in *33rd National Radio Science Conference (NRSC), Aswan, Egypt, February 2–25* (IEEE, 2016), pp. 49–56.